SENSITIVITY AND UNCERTAINTY ANALYSIS FOR FAULT DETECTION IN SOLAR THERMAL SYSTEMS

Corry de Keizer, Klaus Vajen and Ulrike Jordan

Kassel University, Institute of Thermal Engineering, Kassel (Germany)

Abstract

One approach for detecting faults during the operation of solar thermal systems is to compare measured to simulated heat flows in e.g. the secondary solar loop. For detecting faults, it is essential to have knowledge of the uncertainty in both measurements and simulation. Uncertainties in the simulation caused by uncertainties of the system parameters and of measured input data have been analysed. Furthermore a local sensitivity analysis, a minimum-maximum analysis and a Monte Carlo analysis have been carried out that describe the effect of parametric and data uncertainties on the simulated energy yield of typical solar thermal systems. These have been applied to four 'typical' solar thermal systems that are simulated in TRNSYS 17.

1. Introduction

In model-based fault detection, faults are diagnosed by comparing measured and simulated energy yields or other characteristics, however, these values have an unknown error and are therefore uncertain. The 'Guide to the expression of uncertainty in measurement' defines the uncertainty of a measurement as the "parameter, associated with the result of a measurement, that characterizes the dispersion of the values that could reasonably be attributed to the measurand" (JCGM, 2008). For detecting faults it is important to quantify uncertainties of both simulated and measured values (see Figure 1).

The uncertainty of a measurement is not a given fact, but can be influenced by the choice of measurement equipment, or for parameters in the simulation by increasing the effort to get more accurate input data (e.g. pipe length). In long-term monitoring the uncertainties are not limited by technical limits, but by a cost/benefit balance.

The aim of this paper is to study the uncertainties of simulated energy yields of four typical case study systems and to determine how these are most effectively calculated.

In the first section measurement uncertainties, some sensor scenarios and parametric uncertainties are discussed. In the following section a local sensitivity analysis is presented for all four case study systems. The third section considers the simulation uncertainty analysis, in which a minimum-maximum analysis and a Monte Carlo uncertainty analysis are conducted and discussed.

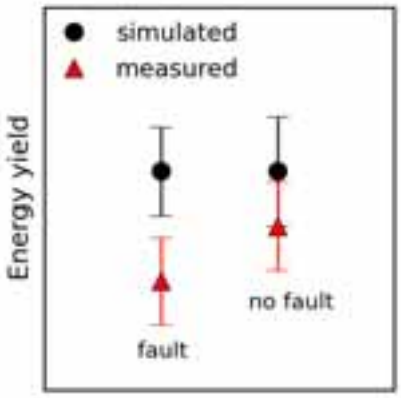

Figure 1: Uncertainty and faults

The sensitivity and uncertainty analyses have been carried out for simulation models of four case study systems: a system that feeds heat into a two-line network (TLN), a system feeding heat into a district heating network (DH), a combi-system (COMBI) and a large domestic hot water system (DHW). The hydraulics and the control strategies of the systems are based on existing systems. One year measured irradiance data in one-minute interval is used as weather input data, the same weather data is used for all the systems. Hot water or heat demand input data was estimated based on measured data. The symplified hydraulics of these four systems are shown in Figure 2.

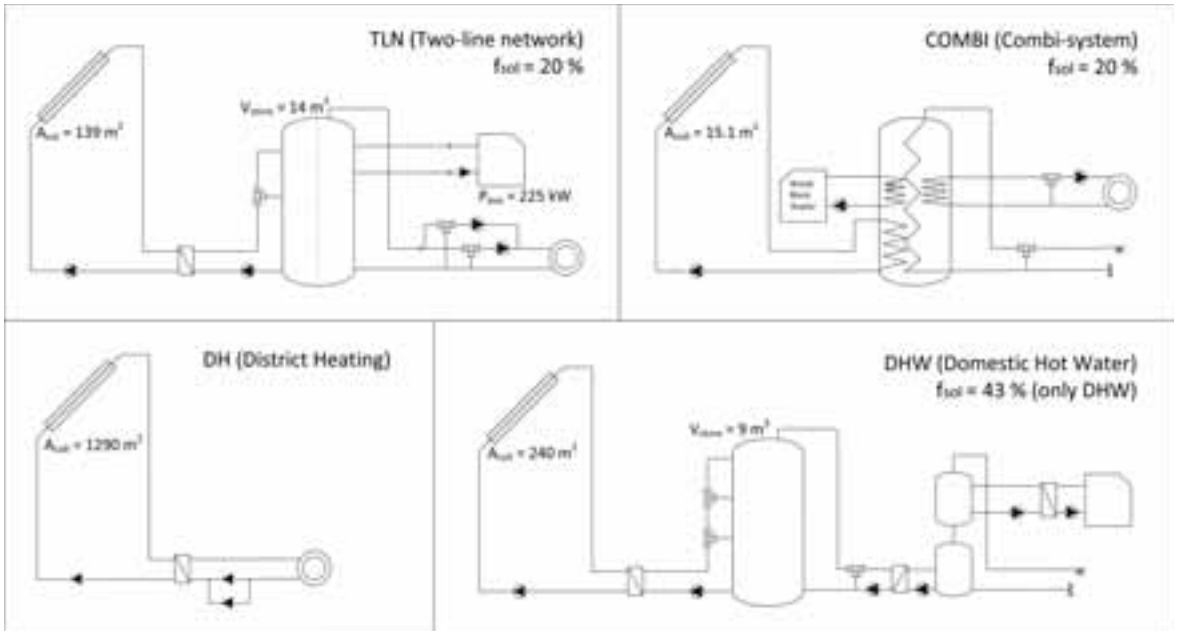

Figure 2: The four case study systems: TLN (Two-line network), DH (District heating), COMBI (Combi-system) and DHW (Domestic Hot Water system)

2. Sensor and parametric uncertainties

2.1 Uncertainties in measurement equipment

Measurement equipment for long-term monitoring and fault detection is usually not the most accurate measurement equipment available, but a compromise between cost and accuracy. In general sensors are not calibrated and resistance temperature sensors are connected in two-lead. To estimate the influence of the accuracy of the measurement equipment, several measurement scenarios with different types of sensor uncertainties have been defined. The sensitivity and uncertainty analyses will show the influence of the different sensors on the simulation uncertainties. Incoming radiation is probably the most influential factor on the solar yield of a solar thermal system, therefore, uncertainties in irradiance measurement have a large influence on the accuracy of the simulation. The daily uncertainties of irradiance sensors in the measurement scenarios are losely based on (Myers and Wilcox, 2009; Düpont and Siemer, 2010), with error margins of 4 % for a CM3 Pyranometer, 5 % for a SP Lite sensor and 8 % for a PV cell. Since at low irradiance levels the relative error is very large, an absolute uncertainty is included and the absolute uncertainty margins are put at 10 W/m^2. The European Norm 60751 defines tolerance classes for temperature sensors A ($\Delta T = 0.15 + 0.002|T|$) and B ($\Delta T = 0.30 + 0.005|T|$), whereby also fractions of tolerance class B may be defined (DIN, 2009-05-01). Errors in the measurement chain, however, remain even if the tolerance of the sensor is defined, e.g. the lead resistance for two-lead measurements, linearisation faults and errors due to conversion processes in the datalogger. An additional uncertainty of 0.3 K is assumed for that. For volume flow sensors (typically multiple jet or turbine flow meters) maximum uncertainty margins of 2 to 3 % are considered.

Table 1: Measurement uncertainty scenarios

Irradiance sensor		Temperature sensor		Volume flow sensor	
Type	**Error Margins (W/m^2)**	**Type**	**Error Margins (°C)**	**Type**	**Error Margins**
CM3	10 +4%	1/3 B	0.4 +0.17 %		
SP Lite	10 +5%	B	0.6 +0.5 %	Cl.2	2%
PV Cell	10 +8%			Cl.3	3%

2.2 Uncertainties in simulation

Uncertainties in the simulation are caused by different factors:

- uncertainty in simulation parameters (e.g. collector efficiency)
- uncertainty of measured input data (e.g. irradiance)
- uncertainty in the model, its components and their combination

Uncertainties in the first two categories can be estimated based on available literature and datasheets of sensors, for the third category of uncertainties this is not possible. To deal with these first two uncertainty categories the following approach has been used: A local sensitivity analysis has been carried out to estimate which parameters are sensitive and need to be included in the uncertainty analysis for the system simulations.

3. Local sensitivity analysis

A local sensitivity analysis was carried out for the 4 simulation models of the case study systems. One-factor-at-a-time is changed, while all other parameters are kept constant at the value of the base case (bc). The response of the output with respect to a change in input has been studied. For every scenario (sc) 365 one-day simulations for every day of the year were run. This enables a comparison of the thermal energy yield for every day, since starting conditions (e.g. temperature distribution in store) are the same. The start temperature distribution in the store is stratified based on the store temperatures in the base case scenario. The aim of this section is to get information on the influence of parameters and to determine which data/parametric values need to be known with a high accuracy. Furthermore, it defines which parameters need to be taken into account for the uncertainty analysis.

Table 2: Sensitivity analysis scenarios

Parameter	**1**[1]	**2**[1]	**3**[1]	**4**[1]	**Scenarios: Input change in parametric or data value**[2]					
G_{tilt} (W/m^2)	x	x	x	x	8% + 10	5% + 10	10 +4%	-4%-10	-5%-10	-8%-10
T_{amb} (°C)	x	x	x	x	0.5 %+ 0.7	2	1	-1	-2	-0.5%-0.7
$\dot{Q}_{inp}$ (kW)	x		x		10%	5%	2.5%	-2.5%	-5%	-10%
$\dot{V}_{inp}$ (l/h)				x	10%	5%	2.5%	-2.5%	-5%	-10%
T_{inp} (°C)	x	x	x	x	0.5 %+ 0.7	0.17 %+ 0.5	2 & 1	-2 & -1	-0.17 %-0.5	-0.5%-0.7
η_0	x	x	x	x	10%	5%	2.5%	-2.5%	-5%	-10%
$C_{p,col}$	x	x	x	x	20%	10%	5%	-5%	-10%	-20%
$UA_{HX,sol,ext}$[5]	x	x	x[4]	x	20%	10%	5%	-5%	-10%	-20%
$l_{pipe,sol}$[5]	x	x	x	x	100%	60%	30%	-30%	-60%	
$\lambda_{pipe,insu}$	x	x	x	x	60%	30%	-30%	-60%		
$\dot{m}_{nom,prim}$	x	x	x	x	20%	10%	5%	-5%	-10%	-20%
$\dot{m}_{nom,sec}$	x	x		x	20%	10%	5%	-5%	-10%	-20%
V_{st}	x	x	x	x	10%	5%	2.5%	-2.5%	-5%	-10%
$V_{st,dhw}$				x	10%	-10%				
$V_{st,aux}$				x	10%	-10%				
$F_{st,hlf}$	x	x	x	x	60%	30%	15%	-15%	-30%	-60%
$UA_{HX,aux,int}$			x		20%	10%	5%	-5%	-10%	-20%
$UA_{HX,sh,int}$			x		20%	10%	5%	-5%	-10%	-20%
$UA_{HX,dhw}$				x	20%	10%	5%	-5%	-10%	-20%
$\dot{m}_{nom,dhw}$				x	20%	10%	5%	-5%	-10%	-20%
$\phi_{prim,glycol}$	x	x		x	0.05	-0.15				
$hyst_{prim,on\&off}$ (K)	x	x	x	x	2	-2				
$hyst_{sec,on\&off}$ (K)	x	x		x	2	-2				
h_{rel} $T_{aux,on}$	x				0.05	-0.05				
$T_{set,aux,on}$(K)	x				2	-2				
$T_{set,aux,off}$ (K)	x				2	-2				

[1] Case study system numbers: *1* TLN, *2* DH, *3* COMBI, *4* DHW
[2] When % is used relative change $\frac{p_{sc}-p_{bc}}{p_{bc}}$ is meant, otherwise the change is absolute $p_{sc} - p_{bc}$
[3] More scenarios for the UA value have been run for systems TLN, DH and DHW for $UA_{HX,sol}$ is 40, 55, 70, 85 W/m_{col}^2K
[4] Internal heat exchanger
[5] Initial base case values UA_{sol} (in W/m^{2}K): TLN 111 , DH 124, COMBI 120, DHW 120.
l_{pipe}/A_{col} in m/m^2: TLN 0.43 , DH 0.097, COMBI 0.99, DHW 0.13.

The one-factor-at-a-time approach is, strictly seen, only valid if the model is linear (Saltelli et al., 2006).

System properties play a role, for the larger deviations of the base case scenario the system behaviour is not linear. Therefore, one cannot represent the sensitivity of a parameter with a single parameter (e.g. % change in output/% change in input) and the values derived should be seen in their local context.

The scenarios of the sensitivity analysis are shown in Table 2, in total 334 scenarios for 27 parametric/input values of the four systems have been explored. For measured data values, the changes are based on expected uncertainties of different measurement equipment. The changes in parametric values (zero-loss efficiency, nominal mass flow etc.) are [4,2,1,-1,-2,-4] times the expected standard deviation. Since all collector uncertainties are strongly correlated, the uncertainty in the zero-loss efficiency was increased and should reflect the aggregated effect of these all. For some parameters only one variation has been implemented to explore the surroundings of certain control settings (e.g. hysteresis).

A selection of the results are presented in Figure 3 based on the change in daily ($\Delta Q_{sol,d}$) or annual ($\Delta Q_{sol,a}$) solar energy yield in comparison to the systems' base case scenario. The solar energy yield is based on the heat flow of the secondary solar loop or, for systems with internal heat exchanger, of the primary loop. The relative change in daily and annual solar energy yield are defined as follows:

$$Q_{sol,a,x}\ (\text{kWh}) = \sum_{d=1}^{365} Q_{sol,d,x} \qquad \text{annual solar energy yield (x is base case (bc) or scenario n (scn))} \tag{1}$$

$$\Delta Q_{sol,a}\ (-) = \frac{Q_{sol,a,scn} - Q_{sol,a,bc}}{Q_{sol,a,bc}} \qquad \text{relative change in annual solar energy yield} \tag{2}$$

$$\Delta Q_{sol,d}\ (-) = \frac{Q_{sol,d,scn} - Q_{sol,d,bc}}{Q_{sol,d,bc}} \qquad \text{relative change in daily solar energy yield} \tag{3}$$

Figure 3 presents the change in annual energy yield (sum of all days) in comparison to the change in input. Two parameters show a very high sensitivity, these are, as expected, the zero-loss efficiency of the collector and the irradiance in the tilted plane. The sensitivity is quite linear in these surroundings for the change in annual energy yield, however, not for the daily one. The sensivities differ per system, this is partially caused by the return flow temperature in the collector loop for η_0 and G_{tilt}, and by the pipe surface per m^2 collector area for the pipe length (Figure 3c). Figure 3d shows the sensitivity of the UA value of the external heat exchanger in the solar loop, the range of change in input value has been extended up to an $UA_{HX,sol}$-value of circa 40 W/m^2K. The change in output is not linear for the UA value if one extends to lower values. The German Norm VDI 6002 (VDI6002) recommends an UA-value of 100 W/m^2K, if this value is much lower, it is a fault and should not be considered for generating an uncertainty limit.

In Figures 3e and 3f the change in simulated daily energy yield for all 365 days are plotted against the base casel daily energy yield for the scenarios of collector efficiency for system TLN and for the irradiance scenarios for system DHW. A change in the input factors has a much larger impact at lower energy yields. Some scattering as a result of stagnation can be seen. If there is no stagnation in the base case, an increasing solar energy yield can cause stagnation and thereby reduce the daily energy yield. With stagnation in the base case, a parameter leading to a lower energy yield may avoid the stagnation.

The following parametric and input values will be taken into account for the uncertainty analysis:

- Irradiance
- Zero-loss collector efficiency
- All input values (volume flow, heat flow, temperature)
- Ambient temperature
- Nominal mass flow in primary and secondary solar loop
- UA value of heat exchanger in solar loop
- Pipe length in collector loop

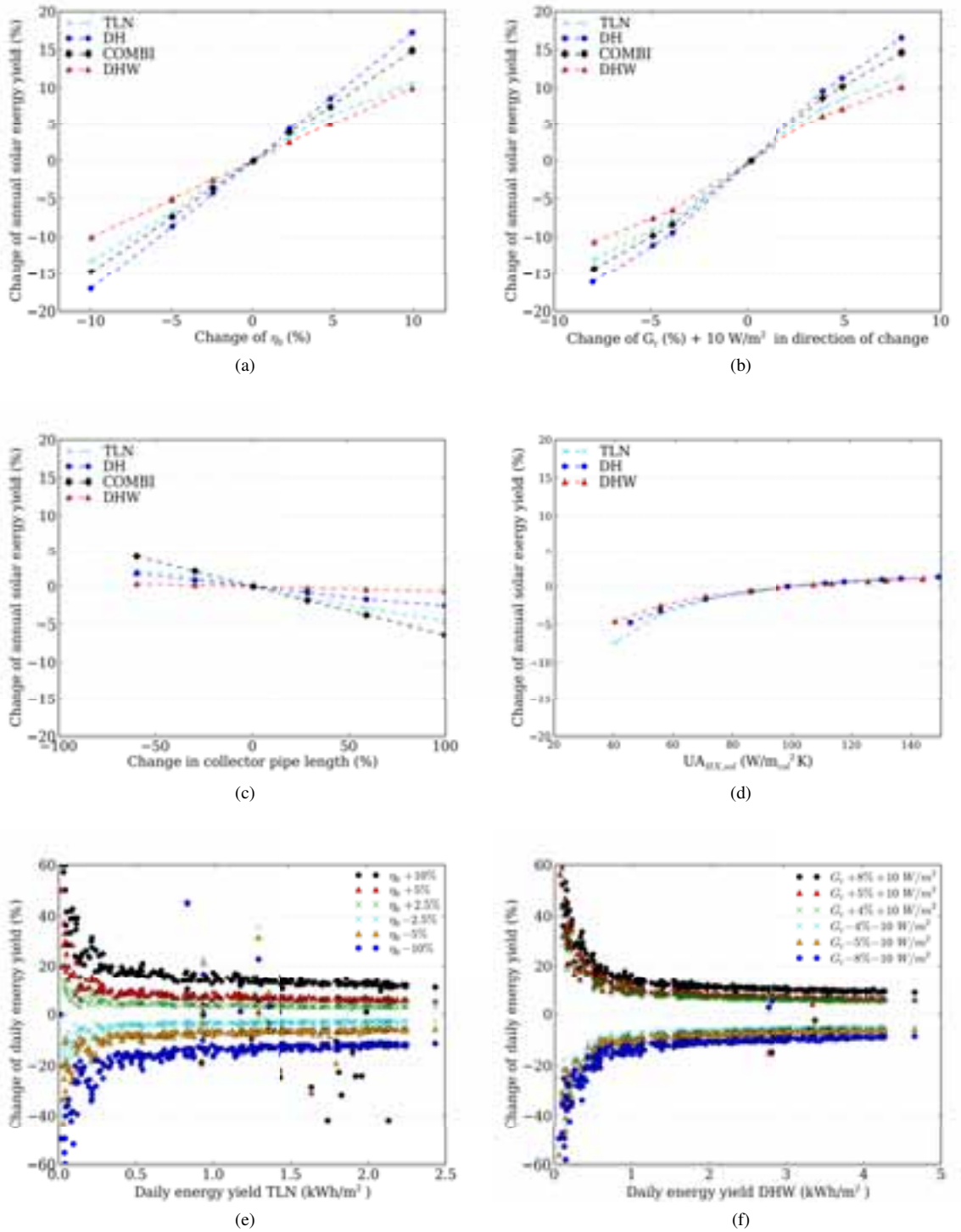

Figure 3: Results of sensitivity analysis, change in output of annual solar energy yield ($\Delta Q_{sol,a}$) (%) for input changes in (a) zero-loss efficiency, (b) irradiation in tilted plane (c) length of pipes in collector loop and (d) UA value of heat exchanger and in output of daily solar energy yield ($\Delta Q_{sol,d}$) (%) of (e) zero-loss efficiency of TLN and (f) irradiation in tilted plane of DHW

4. Uncertainty analysis

4.1 Daily energy yields: Minimum-Maximum (MinMax) approach

The simplest way to calculate a confidence interval for a simulated value is to make two extra simulations for the minimum and maximum value (as done by Wiese (2006)), by putting the sensitive parameters to their maximum or minimum values. Four MinMax-scenarios with different virtual measurement equipment have been carried out for the four case study systems, the changes to the base case input data and parametric values are shown in Table 3.

Table 3: Minimum-maximum scenarios (maximum shown, minimum is -max)

System						Scenario 1		Scenario 2		Scenario 3		Scenario 4		Direction	
1	**2**	**3**	**4**			**rel**	**abs**	**rel**	**abs**	**rel**	**abs**	**rel**	**abs**	***max***	***min***
x	x	x	x	G_{tilt}	W/m^2	5%	10	4%	10	8%	10	5%	10	↑	↓
x	x	x	x	T_{amb}	°C	0.5%	0.6	0.5%	0.6	0.5%	0.6	0.5%	0.6	↑	↓
x	x	x	x	T_{inp}	°C	0.17%	0.4	0.17%	0.4	0.5%	0.6	0.5%	0.6	↓	↑
x		x		Q_{inp}	kW	6%		3%		6%		6%		↑	↓
		x	x	V_{inp}	l/h	3%		2%		3%		3%		↑	↓
x	x	x	x	η_0	-	5%		5%		5%		5%		↑	↓
x	x	x	x	$UA_{HX,sol}$	W/m$^2{}_{col}$K	15%		15%		15%		15%		↑	↓
x	x	x	x	l_{pipe}	m	30%		30%		30%		30%		↓	↑
x	x	x	x	$m_{nom,prim}$	kg/h	3%		3%		3%		3%		↑	↓
x	x		x	$m_{nom,sec}$	kg/h	3%		3%		3%		3%		↑	↓

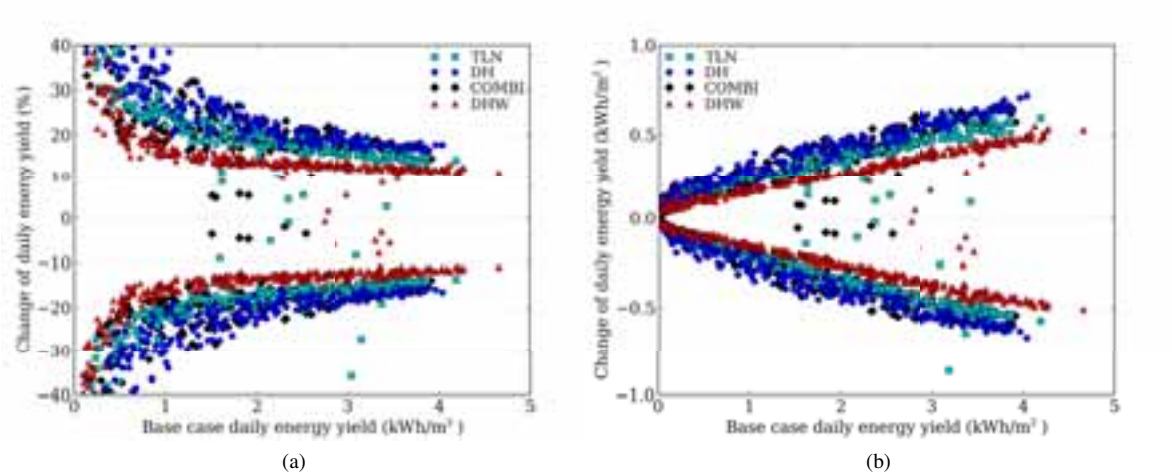

(a) (b)

Figure 4: Results of MinMax Scenario 1, a) relative change in daily solar energy yield ($\Delta Q_{sol,d}$) versus base case specific daily solar energy yield ($Q_{sol,d,bc}/A_{col}$) b) change in daily solar energy yield ($(Q_{sol,d,scn} - Q_{sol,d,bc})/A_{col}$)

The results of scenario 1 are presented in Figure 4, in 4a the relative change of the daily energy yields are presented, while in Figure 4b the absolute changes are shown. It can be seen that the scatter plot of the DHW system follows a much clearer track than the others, furthermore, scattering and the level of change is larger for lower initial energy yields. Some points are scattered outside because of stagnation in the collector loop.

To be able to better interprete the data for different weather circumstances, the resulting data were divided in daily energy yield classes (DEY). The days of the year are split up according to their systems' basecase daily specific solar energy yield ($Q_{sol,d,bc}/A_{col}$) in the following categories: >1, 0.1 < 1, 2 < 3 and > 3 kWh/m^2. The mean change was derived for each DEY and for each scenario by $\sum_e \Delta Q_{sol,e}/ne$, where e represents the days in a specific DEY category and ne is the number of days in e. The mean changes are shown in Table 4 for scenario 1.

The mean change for the max-variant of scenario 1 for daily energy yields larger than 1 kWh/m^2 varies between 13.3 % for system DHW via 17.9 % for system TLN up to 19.9 % for COMBI and 21.2 % for DH. The standard

Table 4: Mean change (%) for maximum-minimum scenarios of the four case study systems

	TLN		DH		COMBI		DHW	
DEY	**s1mx**	**s1mn**	**s1mx**	**s1mn**	**s1mx**	**s1mn**	**s1mx**	**s1mn**
>1	18	-17	21	-20	20	-19	13	-13
0<1	37	-32	45	-41	37	-32	27	-24
1<2	21	-19	25	-23	22	-20	15	-14
2<3	17	-17	20	-19	19	-18	13	-13
>3	15	-15	18	-17	17	-16	12	-12

[1] s = scenario, mn= minimum, mx = maximum
[2] mean change (%) in daily solar energy yield for each DEY
[3] DEY = daily energy yield category, values in kWh/m_{col}^2

deviation of the relative energy yield change represents the width of the scatter in 4a for the specified system, DEY and minimum or maximum and specifies how valid the mean value is for the range of values considered. It ranges from 1.5 % for DHW to 3.9 % for DH. The mean and the standard deviation of the change decrease with larger daily energy yields to 12.2 % for DHW and 17.7 % for system DH with a standard deviation of about 1 %. The change in output for the min-variant of the scenarios are slightly smaller than those for the max-variant, due to the feedback effect, less yield leads to a lower temperature in the storage and a lower mean collector temperature and therefore to a better collector efficiency. In general, the relative error margin in the MinMax analysis is the largest for low daily energy yields.

The minimum-maximum (MinMax) analysis is not methodologically sound, since no probability density function is used for the parameters and the confidence interval of the simulated value is therefore larger than may be necessary. Therefore, in the next section a Monte Carlo Analysis is carried out.

4.2 Daily energy yields: Monte Carlo Analysis

4.2.1 Method

EPA (1997) defines Monte Carlo analysis as a "computer-based method of analysis developed in the 1940's that uses statistical sampling techniques in obtaining a probabilistic approximation to the solution of a mathematical equation or mode". Monte Carlo analysis is often used for uncertainty and sensitivity analyses for non-linear models. In the Monte Carlo analysis all sensitive parameters are varied at the same time by sampling a value out of their probability density function, many simulation trials with sampled parameters are required for getting a stable result. A sample matrix $\mathbf{M}$ is generated for carrying out the Monte Carlo analysis (Saltelli et al., 2006). The matrix has n rows, each row is a trial set for the evaluation of the relative change in the daily energy yield ($\mathbf{y_d}$). Each column represents one parameter, in total r parameters are varied. $\mathbf{y_d}$ is calculated with the TRNSYS model for each row in $\mathbf{M}$ and for each day of the year.

$$\mathbf{M} = \begin{pmatrix} z_{11} & z_{12} & \cdots & z_{1r} \\ z_{21} & z_{22} & \cdots & z_{2r} \\ \vdots & \vdots & \ddots & \vdots \\ z_{n1} & z_{n2} & \cdots & z_{nr} \end{pmatrix}, \boldsymbol{\beta} = \begin{pmatrix} \beta_1 \\ \beta_2 \\ \vdots \\ \beta_r \end{pmatrix}, \mathbf{y_d} = \begin{pmatrix} y_1 \\ y_2 \\ \vdots \\ y_n \end{pmatrix} \tag{4}$$

For practical purposes z_{ij} is defined as the (dimensionless) relative change in parameter p ($z_{ij} = \frac{p_{ij}}{p_0} - 1$), except for the absolute changes, where $z_{ij} = p_{ij}$. Where i represents the number of the trial and j represents the parameter (e.g. G_{tilt}). The relative change in the daily energy yield due the Monte Carlo changes in the parameters for trial i in comparison to the base case is defined as $y_{id} = \frac{Q_{sol,d,i}}{Q_{sol,d,bc}} - 1 \equiv \Delta Q_{sol,id}$. The output results can be assembled in the output matrix $\mathbf{Y}$ with the outputs of the trials in rows, and the days in the different columns.

$$\mathbf{Y} = \begin{pmatrix} y_{11} & y_{12} & \cdots & y_{1,365} \\ y_{21} & y_{22} & \cdots & y_{2,365} \\ \vdots & \vdots & \ddots & \vdots \\ y_{n1} & y_{n2} & \cdots & y_{n,365} \end{pmatrix} \tag{5}$$

Dependent on the case study system, there are up to 15 parametric and input uncertainty values (r). The values for each trial set are randomly sampled based on their probability density function (PDF) that is shown in Table 5, for every day 1000 trial simulations are run (n = 1000). A standard normal distribution was chosen for nearly all parameters, since that is most commonly used and can be defined with only a mean value (μ=0 here) and a standard deviation (σ).

Table 5: Monte Carlo scenario - input uncertainties

System						relative		absolute[1]	
1	**2**	**3**	**4**			σ	**pdf[2]**	σ	**pdf[2]**
x	x	x	x	G_{tilt}	W/m^2	2.5%	normal	10	uniform
x	x	x	x	T_{amb}	°C	0.25%	normal	0.3	normal
x	x	x	x	T_{inp}	°C	0.085%	normal	0.2	normal
x		x		Q_{inp}	kW	3.0%	normal		
		x	x	V_{inp}	l/h	1.5%	normal		
x	x	x	x	η_0	-	2.5%	normal		
x	x	x	x	$UA_{HX,sol}$	W/m$^2_{col}$K	7%	normal		
x	x	x	x	l_{pipe}	m	15%	normal		
x	x	x	x	$m_{nom,prim}$	kg/h	1.5%	normal		
x	x		x	$m_{nom,sec}$	kg/h	1.5%	normal		

[1] The absolute part of the uncertainty is fully correlated to the relative part of the uncertainty by its probability
[2] Assigned probability density function (PDF)

In the Monte Carlo uncertainty analysis the output distribution $\mathbf{y_d}$ is analysed for every day, with regard to the mean value and the standard deviation, and also with regards to the shape of the output distribution. With **M** and **Y** a multilinear regression was carried out (Saltelli et al., 2006) based on the model in Equation 6. With the ordinary least square method, the regression coefficients β_j were determined by minimizing the squares of the residual ε_i. y_{id} the relative change in daily energy yield, due to the change in parameters in trial i in comparison to the base case.

$$y_{id} = \beta_0 + \sum_{j=1}^{r} \beta_j z_{ij} + \varepsilon_i \tag{6}$$

Refsgaard et al. (2005) mentions several advantages and disadvantages of Monte Carlo Analyses. As advantages the gained insight in propagation of uncertainties, the possibility to take any PDF into account as well as correlations and the consequence that analysts need to consider uncertainties explicitly are mentioned. Disadvantages are the limitation to quantifiable uncertainties, the possible lack of information based on which one needs to assign a PDF and the large run time.

4.2.2 Results Monte Carlo global sensitivity analysis

A global sensitivity analysis was conducted by applying a multilinear regression on the results of the Monte Carlo analysis . Least square fitting was implemented for every day and for the daily energy yield classes. The coefficient of determination R^2 is generally larger than 0.95, except for very low energy yields (<0.1 kWh/m^{2}day) and for days with stagnation. The regression coefficients $\boldsymbol{\beta}$ and corresponding R^2 for days without stagnation and a daily energy yield that is larger than 1 kWh/m^2 are shown in Table 6. The larger the β value, the larger the influence on Q_{sol}. To give an example, $\beta_{G_{tilt}}$ for the two-line system (TLN) is 1.35, this means that when G_{tilt} increases 1 %, Q_{sol} increases by 1.35 %.

The corresponding Figure 5 shows the relative change in the daily energy yield (y_{id}) due to Monte Carlo uncertainties versus the ones calculated with regression coefficients ($y_{calc,id} = \beta_0 + \sum_{j=1}^{r} \beta_j z_{ij}$) for the systems DHW and COMBI. Irradiance and zero-loss collector efficiency are the most important factors, causing a change larger than 1% in output per percent change in input. Furthermore the UA-value of the internal heat exchanger for the COMBI system, as well as pipe length and ambient and net temperatures show some significance.

The regression coefficients change with changing energy classes. Therefore, it may be difficult to use these

Table 6: Global sensitivity analysis, regression coefficients β_j for the DEY > 1 kWh/m^2.day

		β_j for DEY>1 kWh/m^2.day				Change caused by parameter x [1]			
		TLN	**DH**	**COMBI**	**DHW**	**TLN**	**DH**	**COMBI**	**DHW**
G_{tilt}	rel	1.35	1.67	1.45	1.04	40%	43%	35%	42%
G_{tilt}	abs	0.00	0.00	0.00	0.00	4%	4%	3%	5%
T_{amb}	rel	0.00	0.00	0.00	0.00	0%	0%	0%	0%
T_{amb}	abs	0.02	0.02	0.02	0.01	3%	3%	5%	3%
T_{net}[2]	rel	0.00	0.00	0.00		0%	0%	0%	0%
T_{net}[2]	abs	-0.01	-0.01	0.00		1%	1%	0%	0%
Q_{net}[2]	rel	0.05		0.02		2%		0%	0%
T_{dhw}	rel			0.02	0.00			0%	0%
T_{dhw}	abs			0.00	-0.01			0%	1%
V_{dhw}	rel			0.03	0.09			0%	2%
η_0		1.36	1.68	1.45	1.04	40%	43%	35%	42%
$UA_{HX,sol}$		0.03	0.03	0.17	0.03	3%	2%	12%	3%
$m_{nom,prim}$		0.00	0.04	0.02	0.03	0%	1%	0%	1%
$m_{nom,sec}$		0.03	0.01		0.00	0%	0%	0%	0%
l_{pipe}		-0.04	-0.02	-0.06	-0.01	6%	4%	8%	1%
β_0		0.00	0.00	0.00	0.00	0%	0%	0%	0%
r^2		**0.98**	**0.96**	**0.98**	**0.99**				

[1] the percentage of the total change caused by parameter j for a scenario in which all parameters are changed by σ (see 5)
[2] For system COMBI 'net' is 'sh' (space heating)

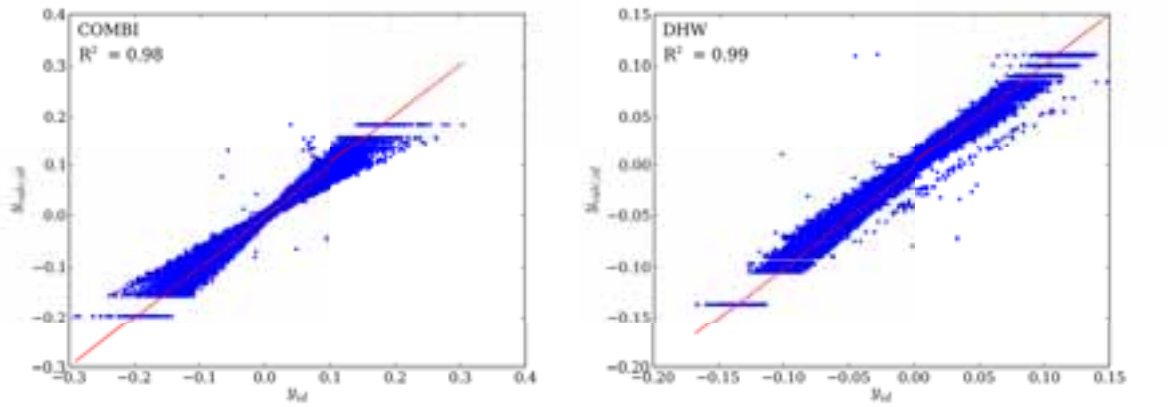

(a) (b)

Figure 5: Relative change in the daily energy yield (y_{id}) versus the with regression coefficients calculated one ($y_{calc,id}$)

for a simple linear calculation of an uncertainty marging around a simulated value. To see how 'good' the fit for the DEY > 1 is for the measured DEY > 3, $y_{calc,id}$ for '>3' was calculated with the regression coefficients of DEY>1. R^2 values are still large and similar to those of DEY>1, so slightly lower than the R^2 for DEY>3 (R^2_{TLN}=0.97, R^2_{DH}=0.96, R^2_{COMBI}=0.98, R^2_{DHW}=0.99).

4.2.3 Results Monte Carlo uncertainty analysis

A summary of the results of the Monto Carlo uncertainty analysis is presented in this section. In Figure 6a a probability plot of the results of 1000 1-day simulations for the DHW system is shown, it resembles a normal distribution. Most of the probability plots for one day resemble this plot, except for days with very low energy yield and those with stagnation. In Figure 6b the results of a day with stagnation for some of the 1000 simulations of system TLN are shown, the standard deviation is therefore much larger than otherwise expected for this system-day combination. The mean daily energy yields and their standard deviations for the daily energy yield classes for days without stagnation are shown in Table 7. Statistically 67 % of the daily energy yields fall within $\mu \pm \sigma$, 95 % within $\mu \pm 2\sigma$ and 99 % within $\mu \pm 3\sigma$. For fault detection one could, for example, decide to use an error margin of 3 σ, for one day, or 2 σ for several days.

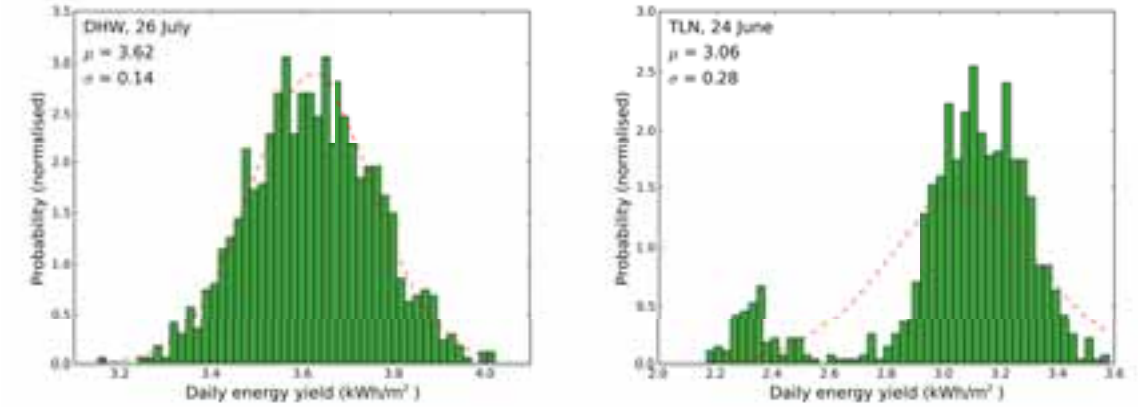

(a) typical distribution result

(b) stagnation

Figure 6: Probability distribution plots of the Monte Carlo analysis for (a) system DHW 26 July and (b) system TLN 24 June with stagnation for some of the trials

Table 7: Mean daily energy yields (kWh/m^2) and standard deviations

	TLN		DH		COMBI		DHW	
DEY	μ	σ	μ	σ	μ	σ	μ	σ
>1	2.45	5.3%	2.44	6.1%	2.21	5.5%	2.62	3.9%
0.1-1	0.54	9.6%	0.54	12.6%	0.54	9.5%	0.56	6.8%
1-2	1.48	6.0%	1.51	7.2%	1.46	6.1%	1.52	4.3%
2-3	2.48	5.2%	2.51	5.8%	2.45	5.3%	2.51	3.9%
>3	3.49	4.7%	3.50	5.2%	3.42	4.9%	3.59	3.6%

4.3 Combination of results and simplification

The minimum and maximum uncertainties derived from the MinMax analysis are compared to the Monte Carlo uncertainties. In theory this is not fully correct, since the probability densitity functions should not be compared to single input values. The comparison shows that for non-stagnation days the minimum and maximum uncertainty values are about 3.2 to 3.6 times larger than the standard deviation derived from the Monte Carlo analysis (for scenario 1 and for the daily energy yield classes). A comparison for every day shows similar values. This means that for our assumed probability density functions the minimum-maximum values can be used as an approximate for the Monte Carlo derived uncertainty distribution. By using the approximation that the mininum or maximum error margin is 3 σ, one would stay on the safe side with a slightly larger σ value than derived in the MC analysis. These results may be different for other input probability density functions.

Nevertheless, for a minimum-maximum simulation, 3 simulations are still necessary for the evaluation of an uncertainty margin. With the regression coefficients (β) it is theoretically possible to calculate the uncertainty margins directly, however, these coefficients differ per system. The calculation of the MinMax values with the regression coefficients for the different DEY categories and systems results in an energy yield difference to the MinMax simulations of ca. 5 %. The factors on which the regression coefficients of η_0 and $G_{tilt,rel}$ depend have been studied, to make it possible to directly state an uncertainty margin. Only $\left(\frac{T_f - T_{amb}}{G}\right)$ showed a correlation with those factors, R^2 was 0.74 for the correlation of the regression coefficients of all systems together for DEY > 1 and for non-stagnation days. These factors determine between 80 and 90 % of the change. Other important factors are $G_{tilt,abs}$, $UA_{HX,sol}$, $T_{amb,rel}$ and l_{pipe}. The regression coefficients of l_{pipe} are correlated with T_{fl} and l_{pipe}/A_{cf}, for the others no correlations were found. The resulting equation to calculate the relative change in the daily energy yield ($y_{simp,d}$) for all systems, depending on the uncertainties of certain parameters is:

$$y_{simp,d} = 1.25\left(22\left(\frac{T_f - T_{amb}}{G}\right)z_G + 22\left(\frac{T_f - T_{amb}}{G}\right)z_{\eta_0} - \left(0.049\left(\frac{l_{\text{pipe}}}{A_{\text{col}}}\right) + 0.00017T_{fl}\right)z_{l_{\text{pipe}}}\right) \quad (7)$$

The results of $y_{simp,d}$ with the MinMax input uncertainties are compared against ΔQ_{sol} of the MinMax simulations. $y_{simp,id}$ is for most systems larger than the average of the absolute Min and Max uncertainty margins (TLN: 4.4 %, DHW: 2.7 %, COMBI 1.5%), except for system DH (DH: -0.9 %). The number of days at which $y_{simp,id}$ is smaller than the average of the absolute Min and Max uncertainty margins differ per system (TLN: 4, DHW: 6, DH: 117, COMBI: 27). Concludingly, Equation 7 generates uncertainty values that are simular to those calculated within the MinMax simulations. The calculated values are in general a bit larger, however, not always, therefore use with care.

5. Discussion and Conclusions

The aim of this paper was to determine the best way to determine TRNSYS simulation uncertainties for fault detection approaches. Two methods were applied a relatively simple minimum-maximum approach and a Monte Carlo Analysis, with which also regression parameters were derived allowing a simple uncertainty calculation. All methods are not suitable on days with stagnation in the collector loop. A strict Monte Carlo analysis is much too time-consuming for general application. The MinMax-approach yields absolute margins that are about 3 to 4 times larger than the standard deviations of the Monte Carlo analysis, so these can be used. The calculations based on general fitted regression coefficients lead to mainly good results, nevertheless, should only be used after more research. There are a few weak points to all these analyses. First of all the limitation to only measured input and simulation parameter uncertainties, leaves out intrinsic TRNSYS uncertainties, as well as other smaller parameter uncertainties or other simulation settings. Secondly sometimes there is lack of information to quantify the uncertainties and to assign a probability density function to those. Nevertheless, even with these limitations the analysis is valuable since it quantifies the effect of measured input and parametric uncertainties on the solar energy yield.

6. Nomenclature

A	(m^2)	Area
C_p	(kJ/K)	Heat capacity
G	($W/m)^2$	Irradiance
l	(m)	Length
$\dot{m}$	(kg/h)	Mass flow rate
Q		Thermal energy yield
$\dot{Q}$	(W)	Heat flow
T	(°C)	Temperature
V	(m^3)	Volume
$\dot{V}$	(l/h)	Volume flow rate

Greek characters

β		regression coefficient
Δ	(-)	Increment, variation
η_0		Zero-loss efficiency
μ		Sample mean
Φ	(-)	volume concentration
σ		Standard deviation

Subscripts / Abbreviations

a	annual
amb	ambient
aux	auxiliary heating loop
bc	base case
col	collector
d	day/daily
DEY	daily energy yield category based on specific solar energy yield of bc (kWh/m^2)
dhw	domestic hot water loop
ext	external

f	fluid (mean flow and return)
f_{sol}	solar fraction ($\frac{Q_{sol}}{Q_{aux}+Q_{sol}}$)
fl	flow
h	height
HX	heat exchanger
hyst	hysteresis
inp	input
insu	insulation
int	internal
nom	nominal
net	local or district heating net
p	parameter
pipe	pipe lines in solar heating loop
prim	primary solar loop
sc	scenario
sec	secondary loop
sol	solar loop
st	store
tilt	in the tilted plane
y	ΔQ_{sol}

Systems

COMBI	Combi
DH	District heating
DHW	Domestic Hot Water
TLN	Two-line network

Acknowledgements

The authors gratefully acknowledge the financial support provided by the Marie Curie early stage Research Training Network 'Advanced solar heating and cooling for buildings - SOLNET' that is funded by the European Commission under contract MEST-CT-2005-020498 of the Sixth Framework Programme. Further financial support was provided by the project IP-Solar. This project is supported by the Austrian Climate and Energy Fund and is carried out as part of the 'Energy of the Future' programme under contract number FFG 815747.

References

DIN. Industrielle Platin-Widerstandsthermometer und Platin-Temperatursensoren (IEC 60751:2008); Deutsche Fassung, 2009-05-01.

R. Düpont and J. Siemer. Solarstrahlungssensoren: Test und Marktübersicht: Wie viel Einstrahlung darf es sein? *Photon Profi*, (12):8–40, 2010.

EPA. Guiding Principles for Monte Carlo Analysis: EPA/630/R-97/001, 1997. URL `http://www.epa.gov/NCEA/pdfs/montcarl.pdf`.

JCGM. Evaluation of measurement data — Guide to the expression of uncertainty in measurement, 2008. URL `http://www.bipm.org/utils/common/documents/jcgm/JCGM_100_2008_E.pdf`.

D. R. Myers and S. Wilcox. Relative Accuracy of 1-Minute and Daily Total Solar Radiation Data for 12 Global and 4 Direct Beam Solar Radiometers. In *Proceedings of American Solar Energy Society Annual Conference*, 2009.

J. C. Refsgaard, J. P. van der Sluijs, A. L. Hojberg, and P. Vanrolleghem. HarmoniCa Guidance Uncertainty Analysis: Report commissioned by European Commission. Brussels, Belgium, 2005.

A. Saltelli, M. Ratto, S. Tarantola, and F. Campolongo. Sensitivity analysis practices: Strategies for model-based inference: The Fourth International Conference on Sensitivity Analysis of Model Output (SAMO 2004) - SAMO 2004. *Reliability Engineering & System Safety*, 91(10-11):1109–1125, 2006.

VDI6002. Solar heating for domestic water: General principles, system technology and use in residential building.

F. Wiese. *Langzeitüberwachung großer solarintegrierter Wärmeversorgungsanlagen*. PhD thesis, Kassel University, Kassel, 2006.